Interplay of Vesicle and Lamellae Formation in an Amphiphilic Polyfluorene-*b*-polythiophene All-Conjugated Diblock Copolymer at the Air−Water Interface

Jin Young Park,[†] Nils Koenen,[‡] Michael Forster,[‡] Ramakrishna Ponnapati,[†] Ullrich Scherf,*[,‡] and Rigoberto Advincula*[,†]

Department of Chemistry and Department of Chemical Engineering, University of Houston, Houston, Texas 77204, USA; Macromolecular Chemistry Group and Institute for Polymer Technology, Bergische Universität Wuppertal, Wuppertal, D-42097, Germany

Received October 30, 2007; Revised Manuscript Received April 26, 2008

ABSTRACT: Interfacial behavior and surface morphology of an amphiphilic, all-conjugated rod−rod diblock copolymer, poly[9,9-bis(2-ethylhexyl)fluorene]-*b*-poly[3-(6-diethylphosphonatohexyl)thiophene] or PF2/6-*b*-P3PHT, were investigated by a combination of Langmuir−Blodgett (LB) techniques, optical spectroscopy, and atomic force microscopy (AFM). For the PF2/6-*b*-P3PHT diblock copolymer aggregates, well-defined gas, liquid-expanded, liquid-condensed, and solid states were observed at the air−water interface. The backbones of the polar P3PHT blocks exhibited an edge-on arrangement which is driven by the pendant alkyl chains with the polar phosphate groups; i.e., the polymer main chain orients parallel to the air/water interface with the planes of the thiophene rings in vertical orientation (edge-on). For comparison of the optical properties, three different LB films (transferred at surface pressures of 5, 15, and 50 mN/m), spin- or drop-cast films, and solutions were investigated. Spectral shifts and intensity changes of UV−vis absorption and photoluminescence emission of the films were correlated to changes of the surface morphology. The emission properties after excitation into the higher-bandgap PF2/6 absorption band were governed by both Förster resonance energy transfer (FRET) and conformational changes within the P3PHT block. The AFM images illustrate the formation of vesicular species and their transition into a monolayer lamellar phase upon increased surface pressure and a correlation of the optical properties and aggregation state at the air/water interface.

Introduction

Conjugated polymers such as polythiophenes (PTs),[1] polyfluorenes (PFs),[2] ladder-type poly(*p*-phenylene)s (LPPPs),[3] poly(phenylene vinylene)s (PPVs),[4] and poly(*p*-phenylene ethynylene)s (PPEs)[5] have been investigated as attractive novel materials for electro-optical devices such as organic photovoltaic cells,[6] organic field effect transistors (OFETs),[7] and organic light-emitting diodes (OLEDs).[8] They can exhibit efficient charge carrier transport properties.[9] However, the charge carrier transport behavior of a conjugated polymer with its individual chemical structure is mainly determined by its solid-state morphology, depending on the intrachain conformation and the resulting interpolymer interactions. Conjugated polymers in solution often show finite persistence lengths and exist as (semi)flexible, disordered coils.[10] Consequently, the disordered solution structure is often transferred to the solid state during "conventional" film formation by drop- or spin-casting, making it difficult to achieve long-range ordering without specific postprocessing treatments due to the initial conformational disorder of the conjugated polymer chains. To overcome this limitation, various assembly methods for conjugated polymers, including layer-by-layer (LBL) self-assembly,[11] the Langmuir−Blodgett (LB) method,[12] and the self-assembly of alternating/block copolymers[13] have been utilized. Several conjugated polymers have been specifically tailored toward a high solid-state order for various device applications.[14] For selected systems, the spectroscopic and charge carrier transport properties could be correlated to conformational changes and the spatial arrangement (2D/3D structure formation) that occurs in the solid state.[15]

For rod−coil block copolymers, depending on the length and solution properties of the blocks, many examples of nanostructure formation have been reported.[16] Only a few studies on synthesis and self-assembly for these class of polymers have been published.[17] π-Conjugated blocks offer the additional possibility to study aggregation phenomena in different environments and aggregation states by optical spectroscopy depending on intrachain conformation and interchain interactions in solution and in the solid state. For many conjugated polymers including PTs and PPEs, an association of the solubilizing alkyl chains at the polymer backbone in bad solvents or the solid state can cause conformational changes, leading to chromic effects (thermo- and solvatochromism).[18]

Polyfluorenes are very suitable blue emitters which have been applied in organic light-emitting diodes (OLEDs) and polymer solid-state lasers owing to their high molecular weights, solid-state photoluminescence quantum yields, and chemical stability.[2a,19] The incorporation of a "kinked" 3,6-carbazole units into polyfluorenes can improve the luminescence properties.[20] Regioregular poly(3-alkylthiophene)s (PATs) as a class of rigid-rod polymers with flexible side chains exhibit a semicrystalline morphology in thin films.[21] Poly(3-hexylthiophene), P3HT, is one of the most investigated conjugated polymers for field effect transistor and solar cell applications. For both applications fields, a high structural and regioregularity as well as high molecular weights are of crucial importance.[22] PATs solvent-induced aggregation phenomena have been observed and studied.[23] In spite of the number of homopolymers and related alternating copolymers reported, PAT-based rod−rod block copolymers remain understudied.[24] Very recently, Scherf et al. have described a first amphiphilic, all-conjugated block copolymer (rod−rod type) which is composed of nonpolar PF and polar

* Corresponding authors. E-mail: scherf@uniwuppertal.de; radvincula@uh.edu.
[†] University of Houston.
[‡] Bergische Universität Wuppertal.

10.1021/ma702402g CCC: $40.75
Published on Web 07/22/2008

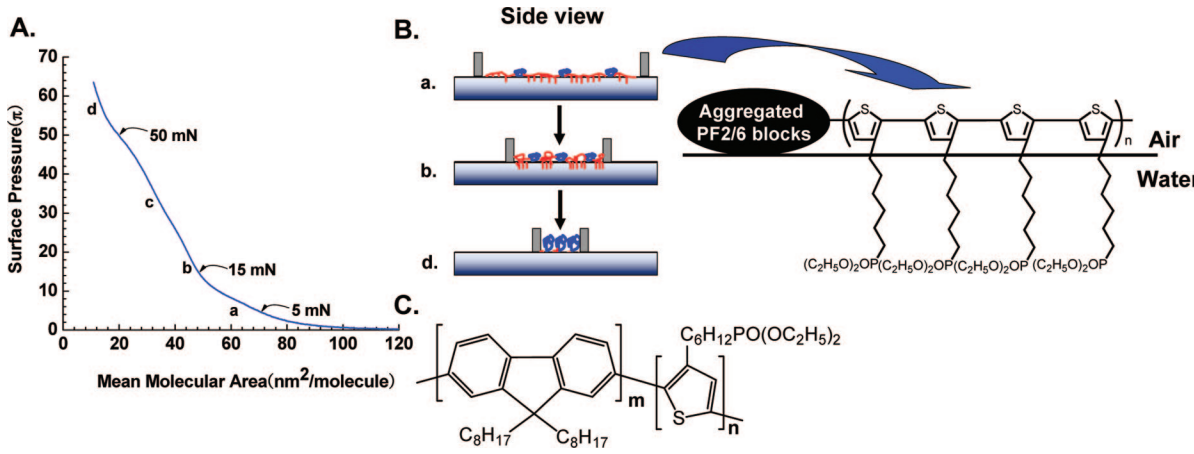

Figure 1. (A) Surface pressure−area (π−A) isotherms of PF2/6-*b*-P3PHT diblock copolymer in $CHCl_3$ (spreading volume: 50 μL, solution concentration: 1 mg/mL). (B) Expected schematic representation at the air−water interface. (C) Chemical structure of PF2/6-*b*-P3PHT.

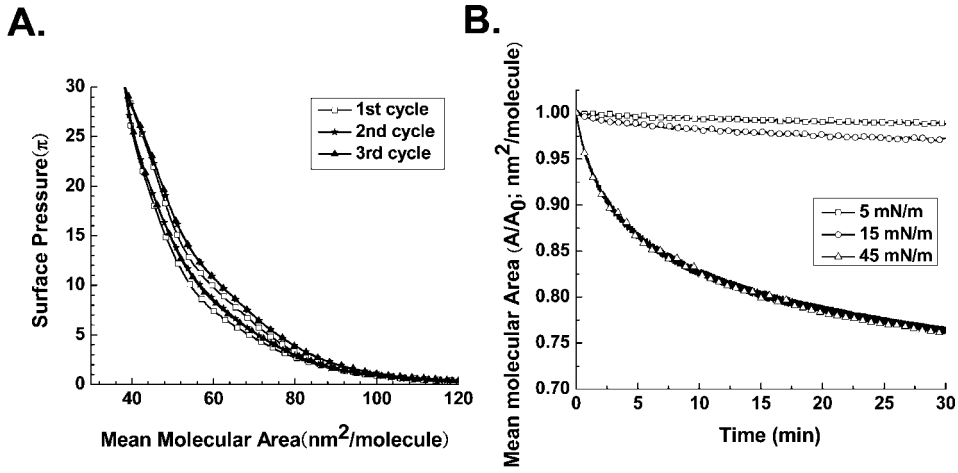

Figure 2. (A) Compression−expansion cycles of amphiphilic PF2/6-*b*-P3PHT LB monolayer at the air−water interface (π_{max}: 30 mN/m). (B) Isobaric measurements at each surface pressure (π = 5, 15, and 45 mN/m) for 30 min.

PAT blocks. Changes in the optical properties in solvent mixtures of selective and nonselective solvents have been reported by this group.[25] They described the formation of supramolecular aggregates in two solvent mixtures (THF/water and THF/hexane) driven by the different polarity and solubility properties of the blocks.

The LB technique should be a powerful method to induce a defined alignment of such rod−rod block copolymers at the air/water interface. The LB technique is a very useful tool to control the assembly of amphiphiles owing to the asymmetry of the air−water interface.[26] Moreover, the morphology of amphiphilic (co)polymers at the air−water interface can be altered as a function of surface pressure, in contrast to conventional film fabrication methods as drop- or spin-casting.

In this work, we report the correlation of surface morphology and optical properties for the amphiphilic, all-conjugated rod−rod block copolymer PF2/6-*b*-P3PHT at the air−water interface. Stability and reversibility of the LB layer formation were investigated by isobaric creep measurements and compression−expansion cycles. The phosphonate side groups on the P3PHT block provide sufficient hydrophilicity for attraction to the water subphase. The hydrophobic polyfluorene (PFs) blocks are expected to be aggregated in the aqueous environment. Obtaining highly oriented films at the air−water interface should be driven by a hierarchic self-assembly of the hydrophilic P3PHT and hydrophobic PF2/6 blocks as well as by surface-pressure-induced phase transitions. Interestingly, the interplay of block copolymer vesicles and monolayer lamellar phase structures have been observed as a function of surface pressure.

Experimental Section

Materials. PF2/6-*b*-P3PHT diblock copolymer (M_w = 62 000 g/mol) was synthesized in a Suzuki-type cross-coupling reaction of 2-bromo-9,9-bis(2-ethylhexyl)fluorene-7-boronic acid in the presence of a monobromo-P3HT macromonomer as end-capper. The detailed synthetic procedure has been reported elsewhere.[25] All solvents ($CHCl_3$ and C_2H_5OH) were of analytical grade purchased commercially from Aldrich Chemical Co. and used without further purification.

Langmuir−Blodgett Film. A KSV-2000 system (KSV Instruments, Finland) was utilized to investigate surface properties and stability of the PF2/6-*b*-P3PHT LB monolayers. The standard trough was cleaned with $CHCl_3$ and C_2H_5OH before pouring Millipore water (resistivity: >18 MΩ·cm, 20 °C). Before adding any spreading solution, several cleaning cycles were done on the LB trough to remove impurities specifically where the two Teflon-coated mobile barriers move inward to maximum position. 50 μL of a copolymer solution prepared by dissolving the PF2/6-*b*-P3PHT in $CHCl_3$ (1.0 mg/mL) was carefully spread with 5−7 μL on each droplet in several spots on the water surface. The solvent was then allowed to evaporate for about 10 min prior to compression. Unless mentioned otherwise, for π−A isotherms and LB deposition the barrier speed was set up at a speed of 5 mm/min (4.2 nm^2/(molecule min)) in all experiments. After each experiment, the initial cleaning procedure was repeated with $CHCl_3$ and C_2H_5OH. For PF2/6-*b*-P3PHT LB deposition, clean BK7 glasses and SiO_2 substrates were

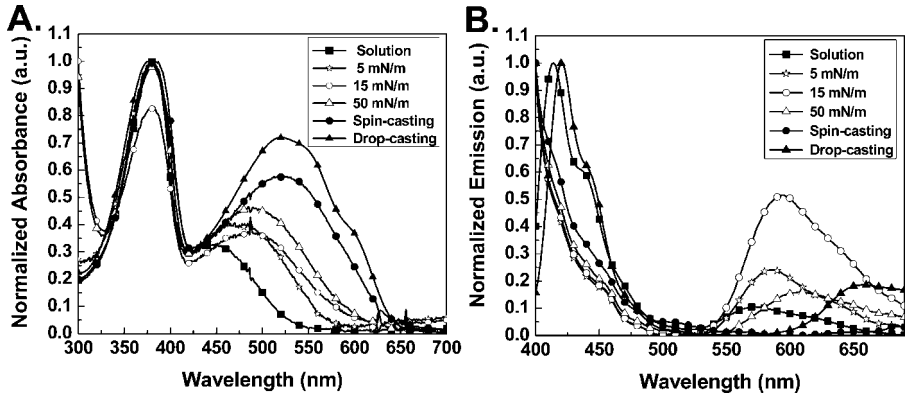

Figure 3. (A) UV/vis absorption and (B) photoluminescence spectra of PF2/6-*b*-P3PHT diblock copolymer LB films (π = 5, 15, and 50 mN/m), spin- and drop-casted films for comparison and in solution (chloroform).

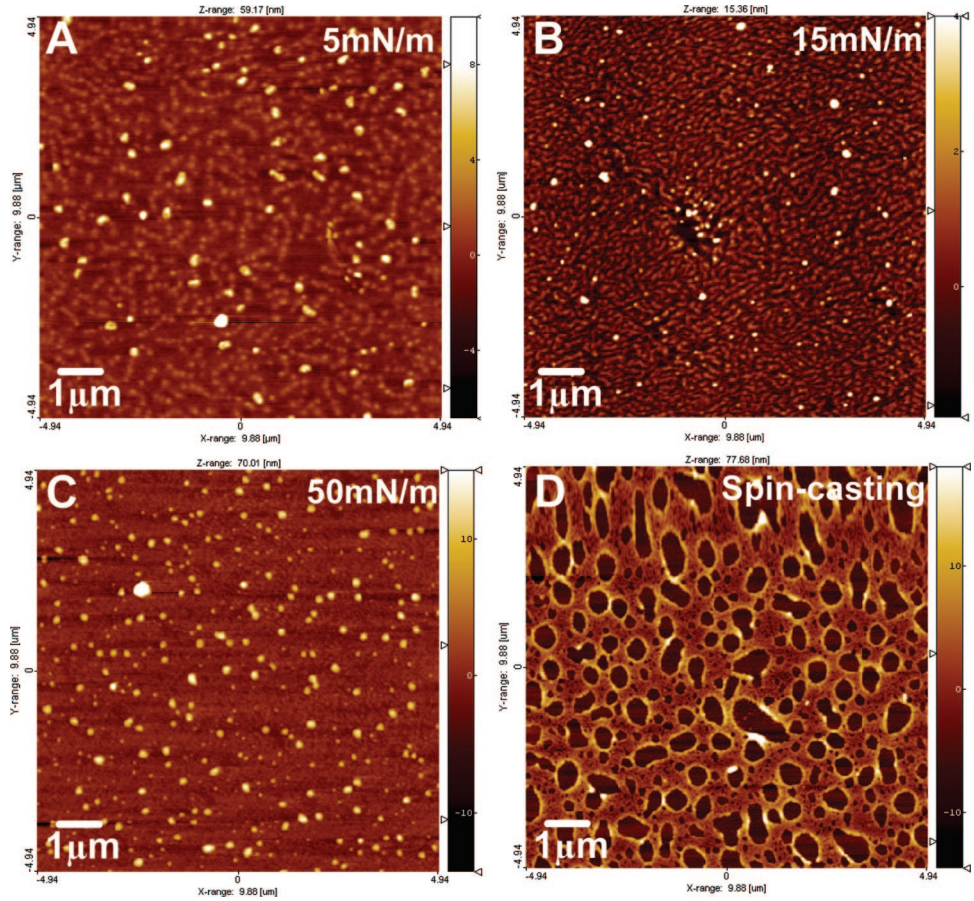

Figure 4. AFM topographic images of PF2/6-*b*-P3PHT LB films transferred at (A) 5, (B) 15, and (C) 50 mN/m and (D) of a spin-casted film. Scan area: 9.88 × 9.88 μm^2.

prepared using the following cleaning procedure: The substrates were sonicated in acetone (15 min), Milli-Q water (15 min), and isopropanol (10 min), dried under a stream of N_2, and then immersed into piranha solution (70/30 by volume H_2SO_4/H_2O_2) (**caution**: strong oxidizing solution) for 50 min. After that, they were washed with H_2O several times and sonicated in isopropanol and Milli-Q water, respectively, and dried in oven at 120 °C. They were kept in a glass jar prior to usage for the LB transfer process. The upstroke speed was 5 mm/min, and LB films were dried under vacuum for a day prior to analysis.

Spectroscopy. UV−vis spectra were recorded using an Agilent 8453 spectrometer. Fluorescence spectra were obtained using a Perkin-Elmer LS45 luminescence spectrometer.

Surface Morphological Measurements. Atomic force microscopy (PICOSCAN SPM, Molecular Imaging Inc., now Agilent 5500 AFM/SPM System (Agilent Technologies)) was used to investigate surface morphologies and surface analysis. The AFM measurements were carried out using a piezoscanner capable of scanning an area of ~10 × 10 μm^2 at room temperature. Commercially available tapping mode tips (TAP300, Silicon AFM Probes, Ted Pella, Inc.) were used on cantilevers with a resonance frequency in the range 290−410 kHz. All images (AFM topography, Tapping mode) were filtered and analyzed by using SPIP software (Scanning Probe Image Processor, Image Metrology A/S). All data in the dimensions of surface aggregates were collected and averaged by at least 20 measurements from line profilometry of the AFM images. Lateral size and height of the aggregate were determined after calibration of AFM tips using a defined patterned surface (MIKRO MASCH, size: 100 nm).

Results and Discussion

***π*−*A* Isotherm.** The surface pressure−area (π−A) isotherm of the amphiphilic PF2/6-*b*-P3PHT diblock copolymer with a

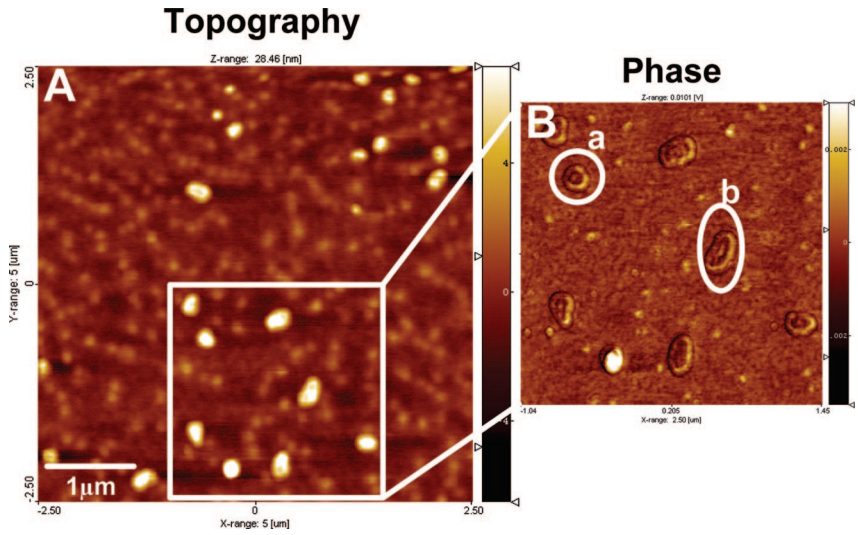

Figure 5. (A) AFM topographic and (B) phase image (zoom-in area in (A)) of the PF2/6-*b*-P3PHT LB films transferred at 5 mN/m at higher magnification. The phase image, in particular, emphasizes the formation of vesicular structures. Scan area: (A) 5.0 × 5.0 μm^2 and (B) 2.5 × 2.5 μm^2.

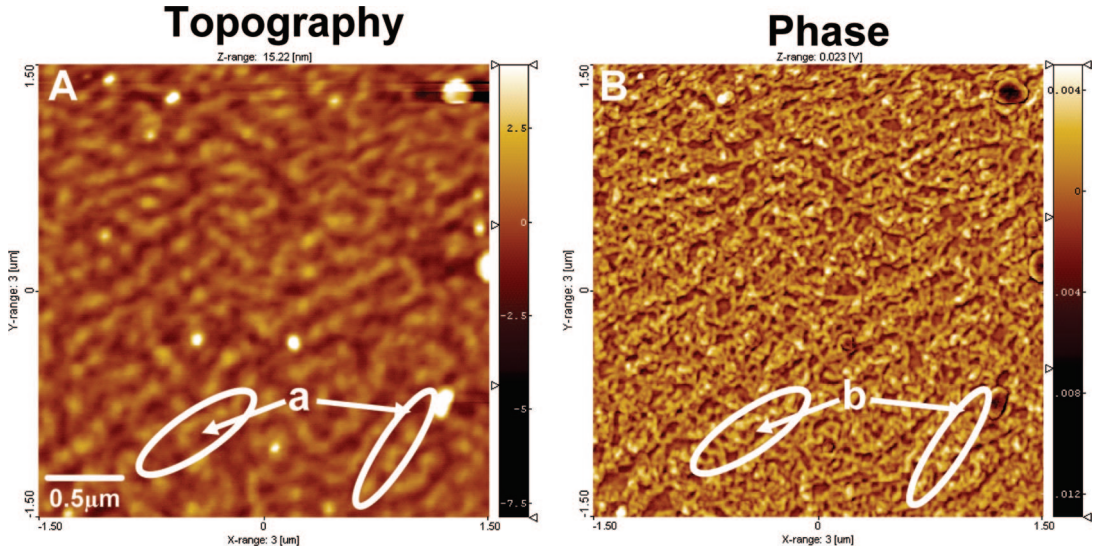

Figure 6. AFM images of PF2/6-*b*-P3PHT diblock copolymer LB film transferred at 15 mN/m at higher magnification (A, topography; B, phase). Scan area: 3 × 3 μm^2.

concentration of 1 mg/mL is shown in Figure 1. The curve was obtained by symmetric compression at a rate of 4.2 nm^2/(molecule min), and the surface pressure was recorded as a function of mean molecular area using a Wilhelmy plate balance. This reproducible $\pi-A$ isotherm shows a typical polymer isotherm behavior,[27] indicating several phases, such as a liquid expanded, a liquid condensed, and a solid state. The initial increase in surface pressure (A_0) gives a mean molecular area of 110 nm^2/macromolecule. In the liquid expanded region (region a), the molecular area decreases dramatically with respect to the increase in surface pressure, reaching up to 12 mN/m due to attractive interaction of the polar phosphonic ester side chains with the water subphase. The limiting area (A_{lim}) is 85 nm^2/macromolecule, as determined by extrapolating the linear part of the $\pi-A$ curve between 4 and 12 mN/m to zero surface pressure. In this liquid expanded region, the limiting virtual area (A_{lim}) can be attributed to face-on polythiophene chain orientation. In the surface pressure region of 12−22 mN/m the monolayer undergoes a pseudo-second-order phase transition probably due to a configurational change to an "edge-on" arrangement of the polythiophene backbones with the pendant phosphonic ester groups oriented toward the water subphase (region b). The observed change in the molecular area per molecule reflects the variation of the angle between the planes of the thiophene rings and the water surface as a function of surface pressure, as shown in previous studies.[28] Distinguishing the dominance of the "face-on" or "edge-on" configuration is important for well-defined molecular order of transferred LB films. Our assumption, hereby, is that the PF2/6 blocks maintain a similar occupied area in this surface pressure region. This is highly probable since the PF2/6 blocks are hydrophobic and already aggregated after the initial spreading of the block copolymer solution at the air−water interface.

With an "edge-on" configuration of the P3PHT chains at the air−water interface, the P3PHT contribution in the Langmuir monolayer should represent the ideal surface area per repeat unit (14.5 $Å^2$) of alkylthiophenes in the solid state.[29] In the condensed state (region c) at surface pressures of 22−50 mN/m, the limiting area is about 60 nm^2/molecule, consistent with densely packed PF2/6 and P3PHT backbones, whereby the plane of the P3PHT backbones adapts an "edge-on" configuration perpendicular to the water surface. In the high surface pressure region (region d), 3-D multilayer structures are expected, implying that a collapse of the initial morphology occurs at the air−water interface. As discussed in the AFM morphology

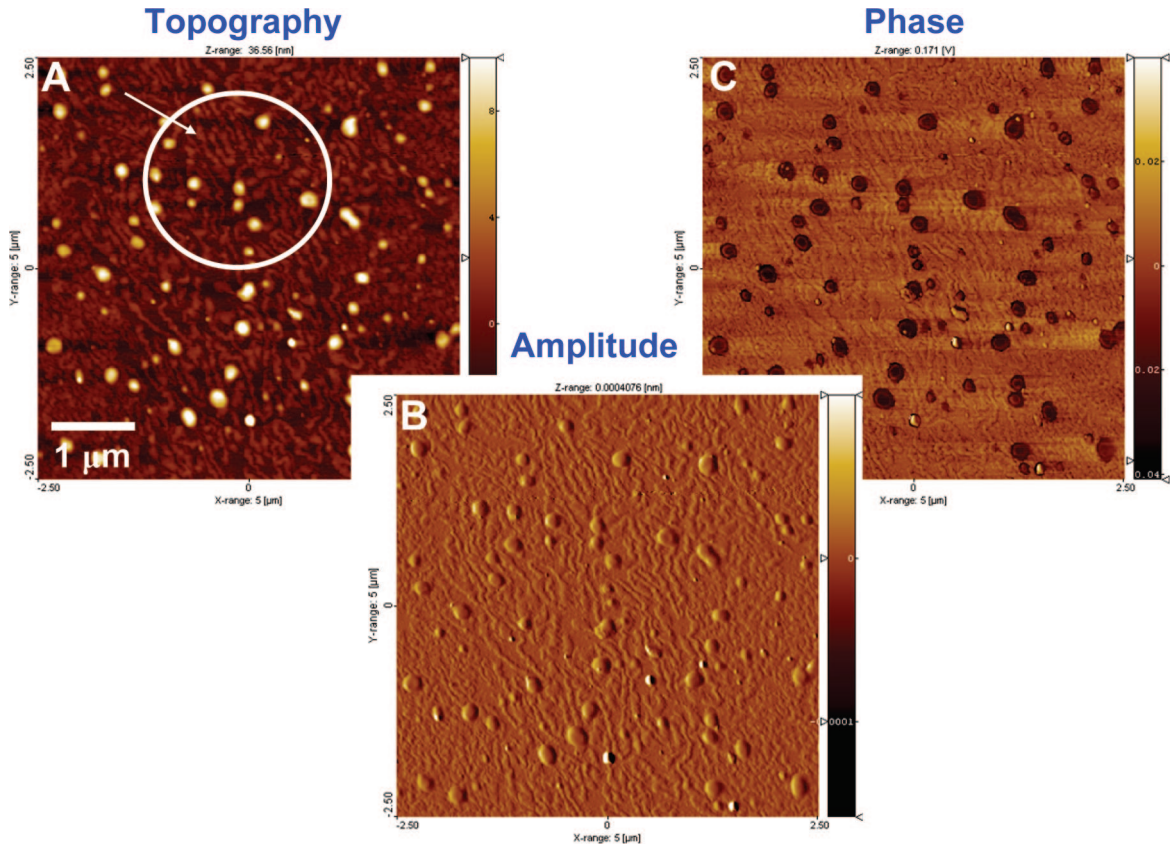

Figure 7. AFM images of PF2/6-*b*-P3PHT diblock copolymer LB film transferred at 50 mN/m at higher magnification (A, topography; B, amplitude; C, phase). Scan area: 5 × 5 μm^2.

Table 1. UV/vis Absorption and Photoluminescence Maxima of PF2/6-*b*-P3PHT

samples		absorption (nm) (UV/vis)	emission (nm) (PL)
films	solution	379, 446	414, 573
	5 mN/m	379, 470	421, 585
	15 mN/m	379, 487	595
	50 mN/m	382, 485	608
	spin-casting	382, 518	
	drop-casting	376, 519	657

section, this actually resulted in the (re)formation of vesicular structures on top of the collapsed monolayers.

Reversibility and Stability. Compression/expansion cyclic experiments, e.g., "hysteresis", have been carried out at the onset point of high surface pressure (π_{max} = 30 mN/m). The monolayer shows very small hysteresis during compression−expansion cycles. After a first compression cycle up to 30 mN/m, the monolayer was decompressed to the maximum area position during expansion process. In Figure 2A the second compression/expansion curve trace is slightly "right"-shifted, indicating the increase in the mean molecular area. It may be due to some reorganization of the initial monolayer formed during/after solvent evaporation at the air−water interface. After the second and third expansion, the surface pressure returns to a very similar area value (at zero surface pressure) as after the first decompression. This phenomenon indicates that the conjugated diblock copolymer essentially shows a reversible monolayer formation behavior at the air−water interface.

Kinetic stability studies of the LB monolayers (isobaric creep measurements) where performed at specified surface pressures (5, 15, and 45 mN/m) for 30 min (Figure 2B). When compressed up to 5 mN/m almost no observable barrier shift occurs, and the change in the mean molecular area (A/A_0 = 0.99) is small. Likewise, in the pseudotransition (π = 15 mN/m; region b) region, the area slightly changed down to A/A_0 = 0.97 and stabilizes within 23 min. However, at high surface pressure (π = 45 mN/m; region c) the film shows unstable behavior at the interface. The mean molecular area decreases rapidly (A/A_0 = 0.77). These observations indicate that at relatively low surface pressures the hydrophilic−lipophilic balance (HLB) of the PF2/6-*b*-P3PHT retains a stable and reproducible arrangement of the block copolymer backbones at the water subphase. Higher surface pressures (ca. 50 mN/m) result in a destabilization/collapse of the Langmuir monolayer.

Optical Properties. The UV/vis spectra of PF2/6-*b*-P3PHT LB films (π = 5, 15, and 50 mN/m) as well as of spin- and drop-cast films are shown in Figure 3A. The higher energy absorption maximum (λ_{max}) at about 380 nm represents the long wavelength absorption peak of the PF2/6 block and the second, lower energy λ_{max} between 440 and 520 nm the absorption peak of the P3PHT block. Absorption and emission of PF2/6 are relatively insensitive to interchain aggregation.[2a] In contrast, the optical properties of regioregular poly(3-alkylthiophene)s as P3HT or P3PHT are very sensitive to intrachain conformational changes and interchain aggregation.[30] In this case, the λ_{max} of the PF2/6 blocks in solution and spin- or drop-casted films are nearly identical. The λ_{max} of the P3PHT block, however, is characterized by a distinct red shift and the occurrence of a structured absorption band in the aggregated state (especially for the drop-casted film with an absorption shoulder around 600 nm), indicating the formation of highly ordered aggregates in the bulk phase. For the three LB films, the absorption λ_{max} of the P3PHT block is generally red-shifted with respect to the solution band and shows an additional red shift of 13 nm with increasing surface pressure. This should be caused by increasing intrachain order and/or interchain interactions with increased compression. This red shift is also a strong evidence of an "edge-

on" configuration of the P3PHT backbones at higher surface pressures which induce an increasing packing density of the planarized P3PHT chains. Similar absorption changes (red-shifted λ_{max} values) of the P3PHT blocks have been also observed in solvent/nonsolvent mixtures, according to an ongoing supramolecular structure formation.[25]

In order to gain further insight into the optical properties, photoluminescence spectra have been recorded under excitation of the PF2/6 absorption band at 380 nm (as shown in Figure 3B). In the PL spectra the two emission bands represent the PF2/6 (blue emission at 400−500 nm) and P3PHT blocks (yellow/red emission at 530−690 nm). The lower energy emission component is generated by Förster-type excitation energy transfer (FRET). The emission peak of the P3PHT block is again red-shifted when going from solution to LB films and shows an additional red shift with increasing surface pressure. In the spin-cast film, the emission band of P3PHT blocks is almost totally quenched. The drop-casted film displays a further red shift of the P3PHT PL band ($\lambda_{max} = 653$ nm). The optical spectra of the LB films indicate an intermediate state between solution and bulk properties. However, orientational effects may influence the optical spectra of the LB films as indicated by increasing absorptions at 300 nm and missing PF2/6 emissions for the LB films at increased surface pressures.

Surface Morphological Change. To investigate the aggregation behavior of PF2/6-*b*-P3PHT (1 mg/mL) with increased surface pressure and to correlate with the optical properties of the transferred LB films, AFM topographic and phase imaging and profilometry were conducted. At low surface pressure ($\pi = 5$ mN/m), the dominant feature of the AFM images are wormlike pearl-necklace structures with the necklace cores formed by the aggregating nonpolar polyfluorene blocks (see Figure 4A). The phase images under higher magnification (Figure 5) and clear images (a and b) confirmed the presence of collapsed vesicles (diameter: 150 ± 30 nm). This indicated the ability of PF2/6-*b*-P3PHT to form vesicular aggregates under LB film manipulation. In agreement with the behavior of typical amphiphilic block copolymers[31] the vesicles should consist of double layers of the amphiphilic, all-conjugated block copolymer with the PF2/6 blocks inside and the polar P3PHT blocks as outer shell. These is likely the case for the vesicles as observed from the phase image (Figure 5b). Spherical aggregates of similar diameters of 120−150 nm have been also observed in solvent/nonsolvent mixtures.[25] On the LB film transferred at 15 mN/m (Figures 4B and 6), the vesicles are no longer visible and must have undergone a transition into the now observed monolayer lamellar morphology (diameters of the lamellar species: 63 ± 11 nm). This morphological transition corresponds to the region of the liquid−liquid transition of the $\pi-A$ isotherm (region b in Figure 1). The root-mean-square ($R_{rms} = 0.764$ nm) roughness of the films dramatically decreases compared to a R_{rms} of 1.49 nm for the LB film transferred at 5 mN/m.

The AFM image of the LB film transferred at 50 mN/m documents a partial reformation of vesicular particles (Figure 4C). These vesicular particles were found to have an average diameter of 110 ± 18 nm. The material underneath the vesicles consists of long-stranded lamellar aggregates which are homogeneously distributed all over the sample (Figure 7A, white circle). The diameter of the lamellar aggregates (69 ± 11 nm) is almost identical to those of the LB films transferred at 15 mN/m. This can be attributed to a closer packing of the PF2/6-*b*-P3PHT chains at higher surface pressure. At the same time, the re-formation of vesicles illustrates the destruction of the monolayers under extrusion of vesicular species from the initial lamellar monolayer to a multilayer domain at or near the collapse pressure.

Our morphology findings can be correlated to the optical properties in terms of an organization and rearrangement of the PF2/6 and P3PHT blocks. An increased surface pressure prior to the transfer of the LB films leads to an increasing amount of lamellar organized monolayers with an increased interchain order and subsequently to an increasing red shift of the P3PHT absorption and emission. Therefore, the interchain order can be "artificially" increased at higher surface pressures. On the contrary, the spin-coated copolymer films (Figure 4D and Figure S1) show dewetting with spherical droplets surrounded by uncoated areas. No lamellar or vesicular features were observed at all, even in the drop-casting film (Figure S2). In the future, it will be ideal to correlate these results with carefully prepared transmission electron microscopy (TEM) experiments with staining in order to further distinguish and characterize block copolymer domains and vesicle formation at various surface pressures.

Conclusions

The aggregation behavior of an amphiphilic, all-conjugated PF2/6-*b*-P3PHT copolymer at the air−water interface was investigated with a combination of LB technique, optical spectroscopy, and AFM. The $\pi-A$ isotherm of the all-conjugated block copolymer shows various 2-D phase states. The LB monolayers are stable up to a surface pressure of ~45 mN/m. Absorption and emission spectra of the LB films transferred at different surface pressures illustrated a continuous packing of the polar polythiophene blocks with different phase transitions. AFM allowed visualization of the initial formation of vesicular species which undergo a fusion to lamellar monolayers at higher surface pressures followed by an irreversible destruction of the monolayers and finally extrusion/reformation of the vesicles. Future experiments will involve further transmission electron microscopy (TEM) correlation on deposited films. We are also currently investigating the relationship of the LB film morphology and the electroluminescence behavior of transferred monolayers for device applications.

Acknowledgment. The American authors gratefully acknowledge the partial funding from the Robert E. Welch Foundation (E-1551), NSF DMR-06-02896, and NSF CHE-03-04807. The German authors thank the Volkswagen foundation for financial support. We also acknowledge technical support from Agilent Technologies and helpful discussions with Tim Fulghum.

Supporting Information Available: Experimental details, AFM characterization, and histogram analysis for the images. This material is available free of charge via the Internet at http://pubs.acs.org.

References and Notes

(1) McCullough, R. D. *Adv. Mater.* **1998**, *10*, 93.
(2) (a) Scherf, U.; List, E. J. W. *Adv. Mater.* **2002**, *14*, 477. (b) Wang, F.; Luo, J.; Yang, K.; Chen, J.; Huang, F.; Cao, Y. *Macromolecules* **2005**, *38*, 2253.
(3) Scherf, U. *J. Mater. Chem.* **1999**, *9*, 1853.
(4) Kulkarni, A. P.; Tonzola, C. J.; Babel, A.; Jenekhe, S. A. *Chem. Mater.* **2004**, *16*, 4556.
(5) (a) Bunz, U. H. F. *Chem. Rev.* **2000**, *100*, 1605. (b) Bunz, U. H. F. *Adv. Polym. Sci.* **2005**, *177*, 1.
(6) (a) Shi, C.; Yao, Y.; Yang, Y.; Pei, Q. *J. Am. Chem. Soc.* **2006**, *128*, 8980. (b) Günes, S.; Neugebauer, H.; Sariciftci, N. S. *Chem. Rev.* **2007**, *107*, 1324. (c) Brabec, C. J.; Sariciftci, N. S.; Hummelen, J. C. *Adv. Funct. Mater.* **2001**, *11*, 15. (d) Kim, J. Y.; Lee, K. H.; Coates, N. E.; Moses, D.; Nguyen, T. Q.; Dante, M.; Heeger, A. J. *Science* **2007**, *317*, 222.
(7) (a) Horowitz, G. *Adv. Mater.* **1998**, *10*, 365. (b) Dimitrakopoulos, C. D.; Malenfant, P. R. L. *Adv. Mater.* **2002**, *14*, 99.
(8) *Organic Light-Emitting Devices*; Müllen, K., Scherf, U., Eds.; Wiley-VCH: Weinheim, 2006.

(9) Hoeben, F. J. M.; Jonkheijm, P.; Meijer, E. W.; Schenning, A. P. H. J. *Chem. Rev.* **2005**, *105*, 1491.
(10) Fytas, G.; Nothofer, H. G.; Scherf, U.; Vlassopoulos, D.; Meier, G. *Macromolecules* **2002**, *35*, 481.
(11) (a) McQuade, D. T.; Hegedus, A. H.; Swager, T. M. *J. Am. Chem. Soc.* **2000**, *122*, 12389. (b) Zhai, L.; McCullough, R. D. *Adv. Mater.* **2002**, *14*, 901.
(12) Bjørnholm, T.; Greve, D. R.; Reitzel, N.; Hassenkam, T.; Kjaer, K.; Howes, P. B.; Larsen, N. B.; Bøgelund, J.; Jayaraman, M.; Ewbank, P. C.; McCullough, R. D. *J. Am. Chem. Soc.* **1998**, *120*, 7643.
(13) Donat-Bouillud, A.; Lévesque, I.; Tao, Y.; D'Iorio, M.; Beaupré, S.; Blondin, P.; Ranger, M.; Bouchard, J.; Leclerc, M. *Chem. Mater.* **2000**, *12*, 1931. (b) Levitsky, I. A.; Kim, J.; Swager, T. M. *J. Am. Chem. Soc.* **1999**, *121*, 1466. (c) Han, X.; Chen, X.; Vamvounis, G.; Holdcroft, S. *Macromolecules* **2005**, *38*, 1114. (d) Jiang, Y. F.; Perahia, D.; Wang, Y. Q.; Bunz, U. H. F. *Macromolecules* **2006**, *39*, 4941.
(14) Reitzel, N.; Greve, D. R.; Kjaer, K.; Howes, P. B.; Jayaraman, M.; Savoy, S.; McCullough, R. D.; McDevitt, J. T.; Bjørnholm, T. *J. Am. Chem. Soc.* **2000**, *122*, 5788.
(15) Kim, J.; Swager, T. M. *Nature (London)* **2001**, *411*, 1030.
(16) (a) Sary, N.; Mezzenga, R.; Brochon, C.; Hadziioannou, G.; Ruokolainen, J. *Macromolecules* **2007**, *40*, 3277. (b) Olsen, B. D.; Segalman, R. A. *Macromolecules* **2006**, *39*, 7078. (c) Liu, J.; Sheina, E.; Kowalewski, T.; McCullough, R. D. *Angew. Chem., Int. Ed.* **2002**, *41*, 329.
(17) Kros, A.; Jesse, W.; Metselaar, G. A.; Cornelissen, J. J. L. M. *Angew. Chem., Int. Ed.* **2005**, *44*, 4349.
(18) DiCésare, N.; Belletéte, M.; Marrano, C.; Leclerc, M.; Durocher, G. *J. Phys. Chem. A* **1999**, *103*, 795.
(19) Klärner, G.; Lee, J. I.; Davey, M. H.; Miller, R. D. *Adv. Mater.* **1999**, *11*, 115.
(20) Xia, C.; Advincula, R. C. *Macromolecules* **2001**, *34*, 5854.
(21) Hugger, S.; Thomann, R.; Heinzel, T.; Thurn-Albrecht, T. *Colloid Polym. Sci.* **2004**, *282*, 932.
(22) (a) Kline, R. J.; McGehee, M. D.; Kadnikova, E. N.; Liu, J.; Fréchet, J. M. J. *Adv. Mater.* **2003**, *15*, 1519. (b) Zen, A.; Pflaum, J.; Hirschmann, S.; Zhuang, W.; Jaiser, F.; Asawapirom, U.; Rabe, J. P.; Scherf, U.; Neher, D. *Adv. Funct. Mater.* **2004**, *14*, 757. (c) Schilinsky, P.; Asawapirom, U.; Scherf, U.; Biele, M.; Brabec, C. J. *Chem. Mater.* **2005**, *17*, 2175. (d) Ma, W.; Kim, J. Y.; Lee, K. H.; Heeger, A. J. *Macromol. Rapid Commun.* **2007**, *28*, 1776.
(23) (a) Kiriy, N.; Jähne, E.; Adler, H. J.; Schneider, M.; Kiriy, A.; Gorodyska, G.; Minko, S.; Jehnichen, D.; Simon, P.; Fokin, A. A.; Stamm, M. *Nano Lett.* **2003**, *3*, 707. (b) Stokes, K. K.; Heuzé, K.; McCullough, R. D. *Macromolecules* **2003**, *36*, 7114.
(24) (a) Liang, Y.; Wang, H.; Yuan, S.; Lee, Y.; Gan, L.; Yu, L. *J. Mater. Chem.* **2007**, *17*, 2183. (b) Asawapirom, U.; Güntner, R.; Forster, M.; Scherf, U. *Thin Solid Films* **2005**, *477*, 48.
(25) Tu, G.; Li, H.; Forster, M.; Heiderhoff, R.; Balk, L. J.; Sigel, R.; Scherf, U. *Small* **2007**, *3*, 1001.
(26) (a) Kim, J. *Pure Appl. Chem.* **2002**, *74*, 2031. (b) Bjørnholm, T.; Hassenkam, T.; Reitzel, N. *J. Mater. Chem.* **1999**, *9*, 1975.
(27) Lopes, S. I. C.; Gonçalves da Silva, A. M. P. S.; Brogueira, P.; Piçarra, S.; Martinho, J. M. G. *Langmuir* **2007**, *23*, 9310.
(28) (a) Mattu, J.; Johansson, T.; Holdcroft, S.; Leach, G. W. *J. Phys. Chem. B* **2006**, *110*, 15328. (b) Callender, C. L.; Caree, C. A.; Daoust, G.; Leclerc, M. *Thin Solid Films* **1991**, *204*, 451.
(29) (a) Yang, S.; Fan, L.; Yang, S. *J. Phys. Chem. B* **2004**, *108*, 4394. (b) Xu, G.; Bao, Z.; Groves, J. T. *Langmuir* **2000**, *16*, 1834. (c) Bao, Z.; Dodabalapur, A.; Lovinger, A. J. *Appl. Phys. Lett.* **1996**, *69*, 4108.
(30) Stokes, K. K.; Heuzé, K.; McCullough, R. D. *Macromolecules* **2003**, *36*, 7114.
(31) Chung, B.; Choi, M.; Ree, M.; Jung, J. C.; Zin, W. C.; Chang, T. *Macromolecules* **2006**, *39*, 684.

MA702402G